Journal of Power Sources 206 (2012) 320–324

Contents lists available at SciVerse ScienceDirect

Journal of Power Sources

journal homepage: www.elsevier.com/locate/jpowsour

Short communication

In situ Raman study on degradation of edge plane graphite negative-electrodes and effects of film-forming additives

Hiroe Nakagawa[a], Yasuhiro Domi[a], Takayuki Doi[a,*], Manabu Ochida[a], Sigetaka Tsubouchi[a], Toshiro Yamanaka[a], Takeshi Abe[b], Zempachi Ogumi[a]

[a] *Office of Society-Academia Collaboration for Innovation, Kyoto University, Gokasho, Uji, Kyoto 611-0011, Japan*
[b] *Graduate School of Engineering, Kyoto University, Nishikyo-ku, Kyoto 615-8510, Japan*

ARTICLE INFO

Article history:
Received 21 November 2011
Received in revised form 25 January 2012
Accepted 25 January 2012
Available online 3 February 2012

Keywords:
Graphite
Edge plane
Raman spectroscopy
Lithium-ion battery
Additives
Vinylene carbonate

ABSTRACT

Structural changes in the surface of edge plane highly oriented pyrolytic graphite (HOPG) electrodes were studied in ethylene carbonate (EC)-based electrolytes by *in situ* Raman spectroscopy. The Raman spectra revealed that the surface crystallinity of graphite was significantly lowered by the initial intercalation and de-intercalation reactions of Li^+. This structural degradation resulted in a sluggish stage transition of Li-GIC in the vicinity of the edge plane in the subsequent potential cycle. On the other hand, when the film-forming additive vinylene carbonate was used in the EC-based electrolyte solution, the crystallinity of the edge plane HOPG was maintained even after potential cycling. In addition, the phase transition of Li-GIC during the 2nd potential cycle proceeded in the same manner as in the initial cycle. Based on the present results, we discuss the suppressive role of film-forming additives on the degradation of the surface structure as it relates to the intercalation mechanism of Li^+.

1. Introduction

Electrochemical intercalation and de-intercalation reactions of Li^+ have been used in the electrodes of lithium-ion batteries. During charging, Li^+ is intercalated into negative electrodes, and is concurrently de-intercalated from positive electrodes. The reverse reactions occur during discharging. The charge and discharge reactions need to take place with high reversibility over 1000 or more cycles in 10–15 years if lithium-ion batteries are to be used in electric-powered vehicles. To improve the cyclability and durability of lithium-ion batteries, it is necessary to understand the degradation mechanism of lithium-ion batteries upon repeated cycling. However, the deterioration that occurs in each cycle is very subtle, and hence it is not always easy to detect irreversible reactions. *In situ* analysis methods, such as *in situ* Raman spectroscopy [1], *in situ* X-ray diffraction (XRD) [2], *in situ* Fourier transform infrared spectroscopy [3] and *in situ* scanning probe microscopy [4], should be useful for detecting such minute irreversible reactions dynamically, compared to *ex situ* measurement techniques. In addition, *in situ* measurement methods enable us to analyze the interior of lithium-ion batteries without exposure to air, whereas the electrochemical reactions of lithium-ion batteries are very sensitive to air.

Li^+ is intercalated into graphite negative-electrodes to form graphite intercalation compounds (GICs) [5]. A distinctive feature of Li–GICs is a staging phenomenon, which is characterized by intercalated layers that are periodically arranged in a matrix of graphite layers. The phase transition of GICs upon charging and discharging has been studied so far by XRD [6–8] and Raman spectroscopy [9,10]. As a result, the variation in the staged structures of GICs with the electrode potential has been elucidated in detail. Li^+ is intercalated through the interface between the graphite electrode and electrolyte solution. Hence, the kinetics of interfacial Li^+ transfer should be influenced more by the surface structure of graphite than by the bulk structure. Laser Raman spectroscopy can detect Raman scattering near the electrode surface, and therefore is useful for investigating the surface crystal structure of electrodes. Hexagonal graphite crystallizes in the D^4_{6h} space group, and has two doubly degenerate Raman active E_{2g} modes at 42 and 1581 cm^{-1} [11]. Our group previously studied variation of the E_{2g} line with the electrode potential by *in situ* Raman spectroscopy [10], and reported that the Raman spectral changes associated with phase transitions occurred reversibly during charge and discharge cycles; the intensity and frequency of the E_{2g} lines at around 1580 cm^{-1} varied with the phase transition of Li–GICs. In addition, the electrode potential upon the electrochemical intercalation of Li^+ was found to be determined by the surface stage of the Li–GICs.

* Corresponding author. Tel.: +81 774384977; fax: +81 774384996.
E-mail address: doi@saci.kyoto-u.ac.jp (T. Doi).

0378-7753/$ – see front matter © 2012 Elsevier B.V. All rights reserved.
doi:10.1016/j.jpowsour.2012.01.141

Discharge capacities of graphite electrodes gradually fade over prolonged charge and discharge cycles. Several possible mechanisms for this fading of capacity have been suggested, such as the exfoliation of graphite layers due to solvent co-intercalation [12,13], electronic isolation of graphite particles [14], and an increase in interfacial resistance [15]. In addition, graphite electrodes are known to undergo structural disordering after prolonged charge and discharge cycles: the intensity of a disorder-induced line, which peaks at about 1360 cm^{-1} in Raman spectra, increases with cycling [16]. The interlayer spacing of graphite expands about 10% in the direction of the *c*-axis with the intercalation of Li^+ [6,17]. Thus, structural disordering would be caused by repeated cycles of expansion and contraction of the crystal structure with the intercalation and de-intercalation of Li^+. Li^+ is intercalated and de-intercalated at edge plane graphite. Hence, a change in the structure of the edge plane should predominantly influence the charge and discharge characteristics of graphite [18]. However, most of previous studies on graphite electrodes have been carried out using granulous graphite, and hence no distinction was made between the edge and basal planes. In the present study, we used edge plane highly oriented pyrolytic graphite (HOPG) as a model graphite electrode, and observed changes in the surface structure during the first few cycles by *in situ* Raman spectroscopy.

2. Experimental

A block of HOPG (Momentive, ZYH, mosaic spread: $3.5 \pm 1.5^\circ$) was used in this study. The size of the HOPG block was 8 mm × 12 mm × 2 mmt. The schematic diagram of an electrochemical cell for *in situ* Raman measurements was shown previously [1]. The HOPG block was clipped between two SUS304 sheets with a hollow square with minimum pressure required for holding it, and used as a working electrode. The electrochemical cell used had an airtight structure, and was equipped with optically flat Pyrex® glass. The edge and basal planes of HOPG were irradiated with a laser beam through the Pyrex® glass to obtain Raman spectra. The distance between the HOPG surface and the Pyrex® glass was minimized at about 1 mm to suppress scattering from electrolytes. The reference and counter electrodes consisted of lithium foil. All potentials in the text reflect V *vs.* Li/Li^+. The electrolyte solutions used were 1 mol dm^{-3} $LiClO_4$ dissolved in a mixture of ethylene carbonate (EC) and diethyl carbonate (DEC) (1:1 by volume) with and without 2wt% of vinylene carbonate (VC, Kishida Chemical). The water content in the solution was less than 20 ppm. The electrochemical cell held about 50 ml of electrolyte solution. The cell was assembled in an argon-filled glove box with a dew point below −80 °C. Electrochemical Li^+ intercalation (charge) and de-intercalation (discharge) at HOPG were carried out by changing the potential; the HOPG electrode was swept from 3.0 to 1.0 V at 0.5 mV s^{-1}, then from 1.0 to 0.1 V at 0.2 mV s^{-1}, and finally from 0.1 to 0.01 V at 0.1 mV s^{-1}. After the electrode was held at 0.01 V for 5 h, the potential was swept in an anodic direction up to 3.0 V. Raman measurements were carried out continuously under potential control. The integration time for each measurement was 90 s, which is very short compared to the total charging and discharging time, and hence spectral changes during each Raman measurement are considered to be negligible. Raman spectra were excited with a 632.81 nm line (50 mW) of a He–Ne laser through an objective lens: 10-powered and 100-powered long-focus objective lenses were used during potential control and before and after potential cycling, respectively. The scattered light was collected in a backscattering (180°) geometry. The Raman spectra were recorded using a spectrometer (Horiba Jobin-Yvon, HR-800) equipped with a multichannel charge coupled device (CCD) detector. All experiments were carried out at an ambient temperature of *ca.* 25 °C.

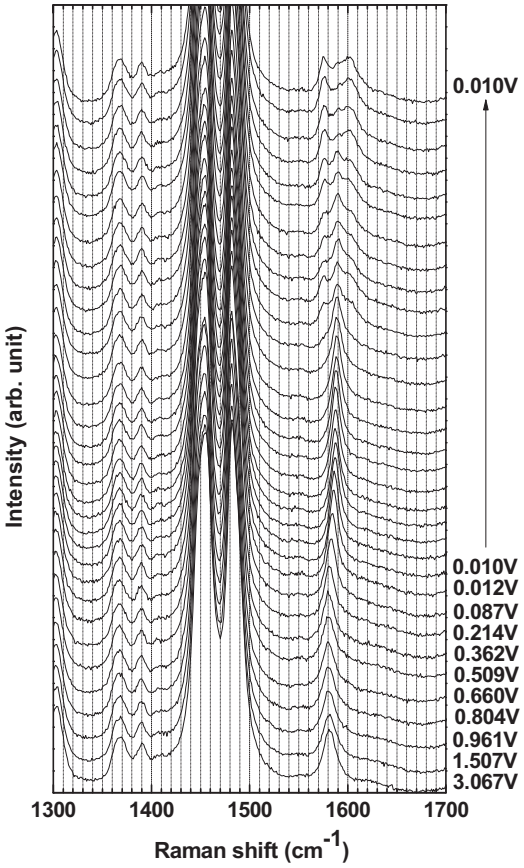

Fig. 1. *In situ* Raman spectra of edge plane HOPG electrode obtained at potentials ranging from 3.0 to 0.01 V in 1 mol dm^{-3} $LiClO_4$/EC + DEC during the initial cathodic polarization.

3. Results and discussion

In cyclic voltammograms of the edge plane HOPG electrode obtained at 0.5 mV s^{-1} (not shown), a cathodic current was seen at potentials below about 1.0 V and a corresponding anodic current was observed at around 1.2 V during anodic scan [18]. These redox currents should be mainly attributed to the intercalation and de-intercalation of Li^+. The voltammogram obtained in the second cycle was very similar to that in the initial cycle. Fig. 1 shows *in situ* Raman spectra of edge plane HOPG at various electrode potentials during a cathodic scan from 3.0 to 0.01 V in 1 mol dm^{-3} $LiClO_4$/EC + DEC. The line that peaks at 1580 cm^{-1} is well known to be related to the crystallinity of carbonaceous materials, and is assigned to the Raman active E_{2g} mode frequency (G band) [11]. The other observed lines were assigned to Raman scattering from solvents and salts in the electrolyte [19]. Variation of the Raman shift of the lines at around 1580 cm^{-1} in the 1st and 2nd potential cycles is summarized in Fig. 2a and b, respectively. The line at around 1580 cm^{-1} gradually shifted toward lower wavenumbers with a decrease in potential, and then shifted toward higher wavenumbers during a cathodic scan down to 0.01 V. In this region, no lines indicative of staged phases were observed. This fact indicates that Li^+ was intercalated randomly between every layer of HOPG; i.e., a dilute stage-1 phase was formed [10,20]. While the electrode potential was held at 0.01 V, the line assigned to dilute stage-1 again broadened, and two lines newly appeared on both sides of the original line, as shown in Figs. 1 and 2a. The new lines were located at about 1575 and 1600 cm^{-1} and the Raman shift hardly changed with time. The intensity of the new lines increased with time, while that of the original line decreased. Based on the

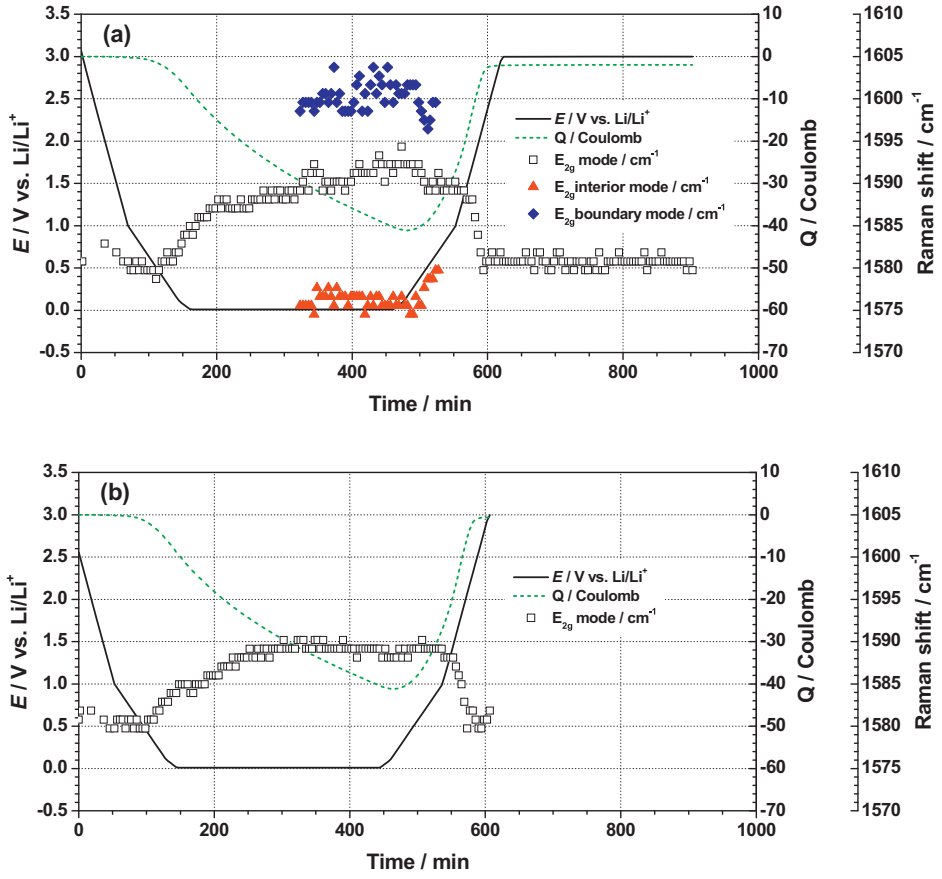

Fig. 2. Variation of the electrode potentials of edge plane HOPG, integrated charge amount, and Raman shift of the lines at around 1580 cm^{-1} with time in the (a) 1st and (b) 2nd potential cycles between 3.0 and 0.01 V. The electrolyte solution used was 1 mol dm^{-3} $LiClO_4$/EC + DEC.

literature, the new lines were assigned to the interior and bounding layer modes of stage-4, *i.e.*, a phase transition from dilute stage-1 to stage-4 occurred [10]. The formation of a dilute stage-1 phase and the subsequent phase transition from dilute stage-1 to stage-4 are known to occur at higher potentials above 0.2 V when a graphite electrode is charged with a constant current at a reasonably slow rate. However, these phase-changes were observed at 0.01 V in this study because of the relatively rapid potential scan.

When the electrode potential was scanned in an anodic direction from 0.01 V, the two lines assigned to stage-4 approached the original line, as shown in Fig. 2a; the lower and upper frequency components shifted towards higher and lower wavenumbers, respectively, and then disappeared at around 0.5 V. These behaviors are different from the nearly unchanged Raman shifts of the two lines during the intercalation of Li^+. Thus, the two lines changed irreversibly during the initial potential cycle, which implies that irreversible changes should occur at edge plane graphite during the intercalation process. This assumption is proven by *in situ* Raman measurements in the second cycle. After the electrode potential was scanned back to 3.0 V, *in situ* Raman measurements were again carried out during the 2nd cycle in the same manner. The amount of charge consumed during the 2nd charge, which was evaluated by integrating the voltammogram, was 41 C. This value was almost the same as that in the initial charge, as shown in Fig. 2a and b. In the 1st cycle, however, the amount of charge consumed irreversibly was evaluated to be 2 C, whereas almost reversible in the 2nd cycle. The charge should be consumed by the formation of a surface film on graphite, particularly in the 1st charge. Therefore, the amount of Li^+ intercalated in the 2nd cycle should be 2 C more than that in the initial cycle. However, the lines indicative of the formation of a stage-4 phase did not appear within the measurement time, and only the shift of the G band was observed, as shown in Fig. 2b. Thus, the phase transition of graphite electrodes was prevented in the 2nd cycle. These results suggest that some significant changes in the crystal structure should occur on edge plane HOPG during the initial potential cycle. This assumption can be examined by considering the spectral changes before and after potential cycling. Fig. 3 shows

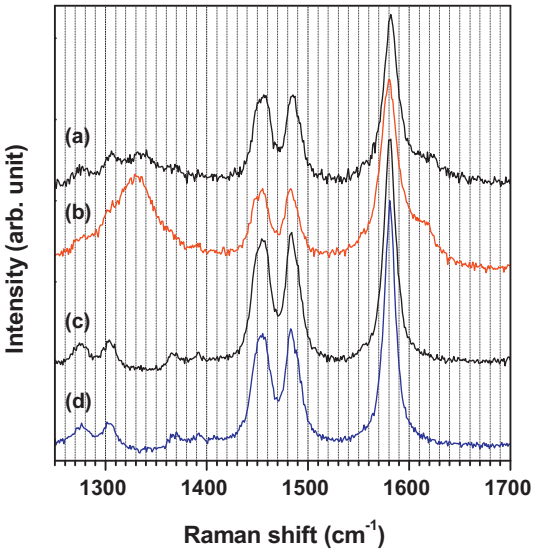

Fig. 3. Raman spectra of edge plane HOPG electrodes (a) before and (b) after potential cycling, and basal plane HOPG electrodes (c) before and (d) after potential cycling. The electrolyte solution used was 1 mol dm^{-3} $LiClO_4$/EC + DEC.

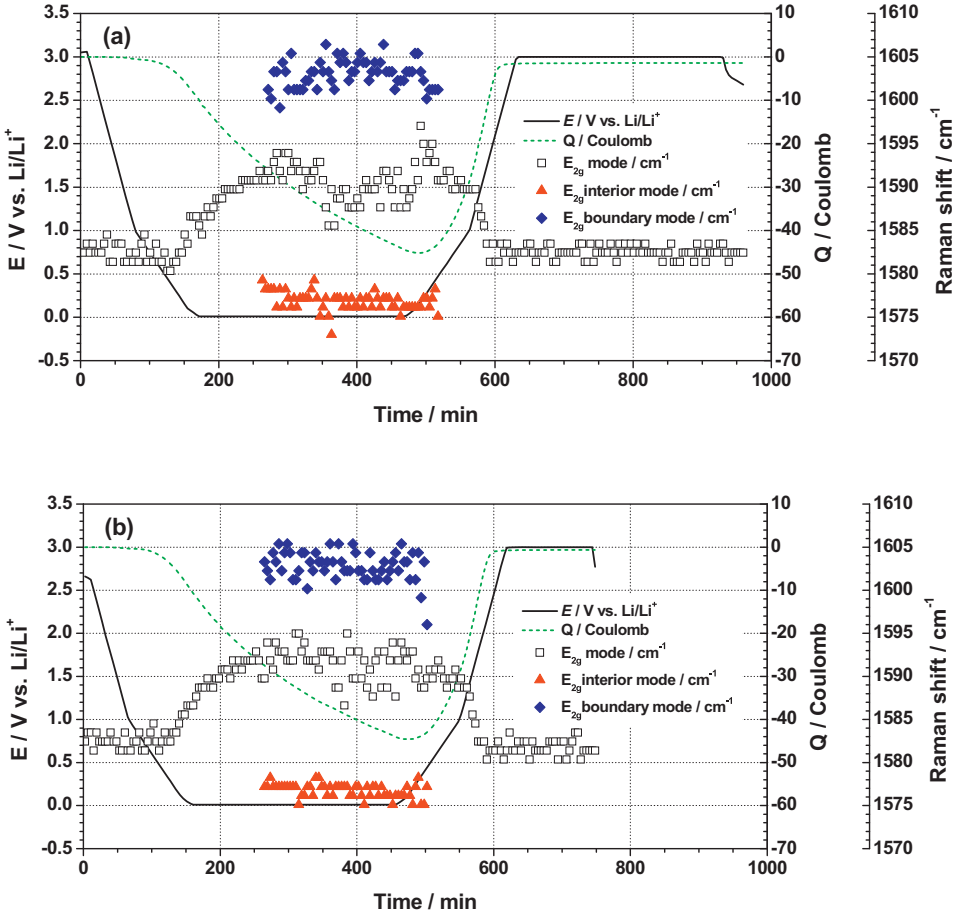

Fig. 4. Variation of the electrode potentials of edge plane HOPG, integrated charge amount, and Raman shift of the lines at around 1580 cm^{-1} with time in the (a) 1st and (b) 2nd potential cycles between 3.0 and 0.01 V. The electrolyte solution used was 1 mol dm^{-3} $LiClO_4$/EC + DEC containing 2 wt% VC.

in situ Raman spectra of the edge plane HOPG electrodes obtained at 3.0 V before and after potential cycling, together with those of the basal plane HOPG electrodes as a reference. After potential cycling, the G band at around 1580 cm^{-1} broadened and two peaks newly appeared at around 1330 and 1620 cm^{-1} for the edge plane HOPG electrodes, as shown in Fig. 3b. The peak at around 1360 cm^{-1} is ascribed to the Raman inactive A_{1g} mode frequency [21]. The peaks at around 1360 (D band) and 1620 cm^{-1} (D′ band) appear in the case of a finite crystal size and imperfections in the carbonaceous materials. On the other hand, such a structural change was not observed for the basal plane HOPG electrodes. These results clearly indicate that the crystallinity of edge plane graphite should decrease with the initial potential cycle. In fact, in Fig. 2a, the Raman shifts of the two lines assigned to stage-4 showed different behaviors under anodic and cathodic polarization, as described above. This fact indicates that the surface crystallinity was already degraded during the intercalation of Li^+.

Drastic expansion of a HOPG electrode, *ca.* 150%, is known to occur at potentials negative than 1.0 V *vs.* Li/Li^+ in EC-based electrolyte solution [22]. Besenhard et al. attributed this expansion to the intercalation of solvated Li^+ [22]. The co-intercalated solvents are subsequently decomposed to form immobile products between the graphite layers, which should serve as a foundation for surface film. This reaction model has been proven by *in situ* scanning tunneling microscopy observation of the step edges on HOPG basal plane [13,23]; when solvated Li^+ is intercalated at 1.1 V, the basal plane in the vicinity of the step edge is raised by about 1 nm, and this is called a hill-like structure. The solvated Li^+ is then decomposed at more negative potentials of *ca.* 0.75 V between graphite layers and the decomposition products result in large swellings with irregular shapes, called blisters. The height of the swellings is approximately 20 nm, which is much higher than the hill-like structures. Since the interlayer spacing of graphite is 0.335 nm, it is not so strange that severe deformation of the crystal lattice should occur upon the formation of hills and blisters in the vicinity of the edge planes. Such a locally drastic expansion of graphite would induce local stresses within graphite layers. These localized stresses might result in irretrievable damage to the host graphite, such as irreversible expansion of the interlayer space, the disordering of carbon atoms, and the breaking of C–C bonds. Thus, degradation of the surface crystal structure of graphite can be expected to occur by the intercalation of solvated Li^+ and/or its subsequent decomposition between graphite layers. This assumption can be proven by the use of film-forming additives in electrolyte solutions. Additives, such as vinylene carbonate (VC) [24], ethylene sulfite (ES) [25] and fluoroethylene carbonate (FEC) [26], are known to be reductively decomposed on a graphite surface to form a passivating surface film. These reactions take place at relatively high potentials of around 1.1 V, and therefore the co-intercalation of EC and DEC should be suppressed. In fact, no evidence for solvent co-intercalation was observed by *in situ* AFM [27]; the hill and blister structures did not appear in electrolytes containing VC, ES, or FEC. Fig. 4a and b show variation of the Raman shift of the lines at around 1580 cm^{-1} in the 1st and 2nd potential cycles, respectively. With the addition of VC to the electrolyte, *in situ* Raman spectra obtained in the 2nd potential cycle were very similar to those in the initial cycle; the lines indicative of the phase formation of dilute stage-1 and the subsequent phase transition from dilute stage-1 to stage-4

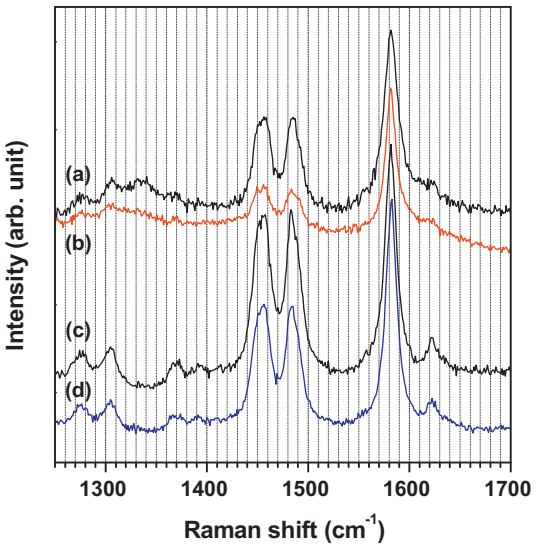

Fig. 5. Raman spectra of edge plane HOPG electrodes (a) before and (b) after potential cycling, and basal plane HOPG electrodes (c) before and (d) after potential cycling. The electrolyte solution used was 1 mol dm^{-3} $LiClO_4$/EC + DEC containing 2 wt% VC.

were observed even in the 2nd cycle. Fig. 5 shows *in situ* Raman spectra of the HOPG edge plane obtained at 3.0 V before and after potential cycling in EC + DEC-based electrolyte solution containing VC. No line indicative of the D and D′ bands appeared after the 1st potential cycle. These results clearly indicate that the surface crystallinity can be maintained even after the intercalation of Li^+. Therefore, the above assumption is clarified to be valid. Based on the present results, film-forming additives not only provide a superior surface film on graphite electrodes, but also play an important role in maintaining the crystal structure of the graphite surface during charge and discharge reactions.

4. Conclusion

The changes in the surface crystallinity of edge plane HOPG were observed by *in situ* Raman spectroscopy under potential control in 1 mol dm^{-3} $LiClO_4$ dissolved in a mixture of EC and DEC with and without the addition of VC. Raman spectra revealed that the surface crystallinity of the edge plane HOPG significantly lowered within only a single charge/discharge cycle when no additives were used. In addition, the phase transition of Li–GIC upon Li^+ intercalation was more sluggish in the 2nd cycle than in the 1st cycle. On the other hand, when an electrolyte solution containing VC was used, the crystal structure of edge plane HOPG was maintained even after potential cycling. In addition, the stage transition of Li–GIC during the 2nd potential cycle proceeded in the same manner as in the 1st cycle. Based on the present results and a consideration of the intercalation mechanism of Li^+, the structural degradation of the graphite surface should be caused by severe deformation of the crystal lattice upon the co-intercalation of solvent molecules. Degradation of the crystal structure of edge plane graphite should result in the sluggish stage transition of Li–GIC in the subsequent charge and discharge cycle. The slow charge and discharge reactions should result in low rate capability and small reversible capacities. Therefore, to improve the charge–discharge characteristics of graphite negative-electrodes, further studies are needed to identify solvent systems or additives that can suppress the co-intercalation of solvent molecules.

Acknowledgements

This work was supported by the New Energy and Industrial Technology Development Organization (NEDO) under contract from the Research & Development Initiative for Scientific Innovation of New Generation Batteries (RISING).

References

[1] M. Inaba, H. Yoshida, Z. Ogumi, J. Electrochem. Soc. 143 (1996) 2572.
[2] D. Aurbach, Y. Ein-Eli, J. Electrochem. Soc. 142 (1995) 1746.
[3] R. Imhof, P. Novák, J. Electrochem. Soc. 145 (1998) 1081.
[4] D. Aurbach, Y. Cohen, J. Electrochem. Soc. 143 (1996) 3525.
[5] A. Herold, Bull. Soc. Chim. Fr. 187 (1955) 999.
[6] J.R. Dahn, Phys. Rev. B 44 (1991) 9170.
[7] T. Ohzuku, Y. Iwakoshi, K. Sawai, J. Electrochem. Soc. 140 (1993) 2490.
[8] Z. Jiang, M. Alamgir, K.M. Abraham, J. Electrochem. Soc. 142 (1995) 333.
[9] P.C. Eklund, G. Dresselhaus, M.S. Dresselhaus, J.E. Fischer, Phys. Rev. B 21 (1980) 4705.
[10] M. Inaba, H. Yoshida, Z. Ogumi, T. Abe, Y. Mizutani, M. Asano, J. Electrochem. Soc. 142 (1995) 20.
[11] R.J. Nemanich, G. Lucovsky, S.A. Solin, Solid State Commun. 23 (1977) 117.
[12] J.O. Besenhard, H.P. Fritz, J. Electroanal. Chem. Interfacial Electrochem. 53 (1974) 329.
[13] M. Inaba, Z. Siroma, A. Funabiki, Z. Ogumi, Langmuir 12 (1996) 1535.
[14] D. Aurbach, M.D. Levi, E. Levi, A. Schechter, J. Phys. Chem. B 101 (1997) 2195.
[15] D. Aurbach, B. Markovsky, A. Rodkin, M. Cojocaru, E. Levi, H.-J. Kim, Electrochim. Acta 47 (2002) 1899.
[16] R. Kostecki, F. McLarnon, J. Power Sources 119–121 (2003) 550.
[17] J.R. Dahn, R. Fong, M.J. Spoon, Phys. Rev. B 42 (1990) 6424.
[18] Y. Domi, M. Ochida, S. Tsubouchi, H. Nakagawa, T. Yamanaka, T. Doi, T. Abe, Z. Ogumi, J. Phys. Chem. C 115 (2011) 25484.
[19] B. Klassen, R. Aroca, J. Phys. Chem. B 102 (1998) 4795.
[20] G.L. Doll, P.C. Eklund, J.E. Fischer, Phys. Rev. B 36 (1987) 4940.
[21] F. Tuinstra, J.L. Koenig, J. Chem. Phys. 53 (1970) 1126.
[22] J.O. Besenhard, M. Winter, J. Yang, W. Biberacher, J. Power Sources 54 (1995) 228.
[23] S.-K. Jeong, M. Inaba, T. Abe, Z. Ogumi, J. Electrochem. Soc. 148 (2001) A989.
[24] B. Simon, J.P. Boeuve, B. Spigai, M. Broussely, Electrochem. Soc. 97–2 (1997) 184, Fall Meeting, Paris, Extended abstracts.
[25] G.H. Wrodnigg, J.O. Besenhard, M. Winter, J. Electrochem. Soc. 146 (1999) 470.
[26] R. McMillan, H. Slegr, Z.X. Shu, W. Wang, J. Power Sources 81–82 (1999) 20.
[27] S.-K. Jeong, M. Inaba, R. Mogi, Y. Iriyama, T. Abe, Z. Ogumi, Langmuir 17 (2001) 8281.